Compact, Low Insertion-Loss, Sharp-Rejection, and Wide-Band Microstrip Bandpass Filters

Lung-Hwa Hsieh, *Student Member, IEEE,* and Kai Chang, *Fellow, IEEE*

***Abstract*—This paper presents a new compact, low insertion-loss, sharp-rejection, and wide-band microstrip bandpass filter. A bandstop filter is introduced that uses a ring resonator with direct-connected orthogonal feed lines. A new bandpass filter based on the bandstop filter uses two tuning stubs to construct a wide-band passband with two sharp stopbands. Without coupling gaps between feed lines and rings, there are no mismatch and radiation losses between them and, therefore, the new filters show low insertion loss. In addition, a dual-mode characteristic is used to increase the stopband bandwidth of the new filters. A simple transmission-line model used to calculate the frequency responses of the filters shows good agreement with measurements. The filter using three cascaded rings has 3-dB fractional bandwidth of 49.3%, an insertion loss of better than 1.6 dB in the passband, a return loss of larger than 13 dB from 4.58 to 7.3 GHz, and two rejections of greater than 40 dB within 2.75–4.02 and 7.73–9.08 GHz. The high-performance, compact-size, and low-cost filter was designed for reducing the interference in full duplex systems in satellite communications.**

***Index Terms*—Bandstop filter, dual mode, ring resonator, wide-band bandpass filter.**

I. Introduction

HIGH performance, compact size, and low cost are highly desirable for modern microwave filters in the next generation of many wireless systems. The microstrip ring resonator satisfies these demands and is finding wide use in many bandpass filters [1]. However, the conventional end-to-line coupling structure of the ring resonator suffers from high insertion loss [2]. The coupling gaps between the feed lines and resonator also affect the resonant frequencies of the resonator. To reduce the high insertion loss, filters used an enhanced coupling structure or lumped capacitors were proposed [3]–[7]. However, the filters using this enhanced coupling structure still have coupling gaps. In addition, the filters using lumped capacitors are not easy to fabricate. Ring resonators using a high temperature superconductor (HTS) to obtain a very low insertion loss have been reported [8]. This approach has the advantage of very low conductor loss, but requires a complex fabrication process.

In this paper, a new compact low insertion-loss sharp-rejection wide-band microstrip bandpass filter is proposed. The wide bandpass filter is developed from a new bandstop filter introduced in Section II. Two tuning stubs are added to the bandstop filter to create a wide passband. In addition, to widen the stopbands, a dual-mode characteristic is used. Without coupling gaps between feed lines and rings, there are no mismatch and radiation losses between them. Thus, the new filter can obtain a low insertion loss [9] and the major losses of the filter are contributed by conductor and dielectric losses. A simple transmission-line model is used to calculate the frequency responses of the filters. The measurements show good agreement with the calculations.

Manuscript received July 28, 2002; revised November 25, 2002. This work was supported in part by the Boeing Company.

The authors are with the Department of Electrical Engineering, Texas A&M University, College Station, TX 77843-3128 USA (e-mail: welber@ee.tamu.edu; chang@ee.tamu.edu).

Digital Object Identifier 10.1109/TMTT.2003.809643

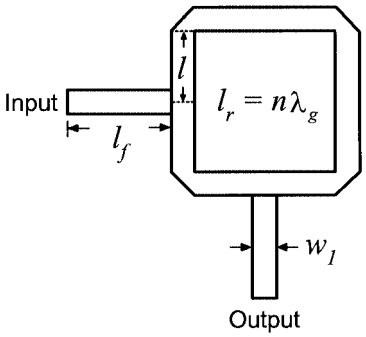

Fig. 1. Ring resonator using direct-connected orthogonal feeders.

II. Bandstop and Bandpass Filters Using a Single Ring With One or Two Tuning Stubs

A. Bandstop Characteristic

The bandstop characteristic of the ring circuit can be realized by using two orthogonal feed lines with coupling gaps between the feed lines and ring resonator [1]. For odd-mode excitation, the output feed line is coupled to a position of the zero electric field along the ring resonator and shows a short circuit [10]. Therefore, no energy is extracted from the ring resonator, and the ring circuit provides a stopband. A ring resonator directly connected to a pair of orthogonal feed lines is shown in Fig. 1. No coupling gaps are used between the resonator and feed lines. The circumference l_r of the ring resonator is expressed as [1]

$$l_r = n\lambda_g \tag{1}$$

where n is the mode number and λ_g is the guided wavelength. In order to investigate the behavior of this ring circuit, an elec-

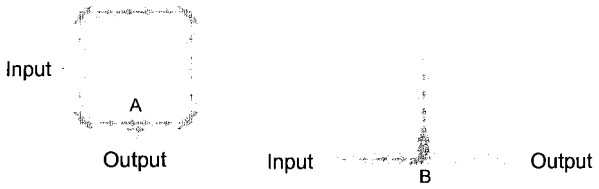

Fig. 2. Simulated electric current at the resonant frequency for the ring and open stub bandstop circuits.

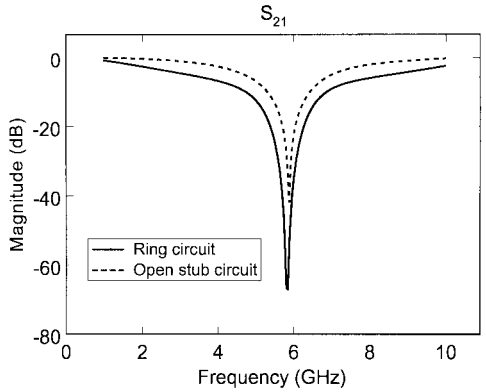

Fig. 3. Simulated results for the bandstop filters.

tromagnetic (EM) simulator[1] and a transmission-line model are used.

Fig. 2 shows the EM simulated electric current distribution of the ring circuit and a conventional $\lambda_g/4$ open-stub bandstop filter at the same fundamental resonant frequency. The arrows represent the electric current. The simulated electric current shows minimum electric fields at positions A and B, which correspond to the maximum magnetic fields. Thus, both circuits provide bandstop characteristics by presenting zero voltages to the outputs at the resonant frequency that can be observed by their simulated frequency response of S_{21}, as shown in Fig. 3. The ring resonator and conventional $\lambda_g/4$ open-stub bandstop filter are designed at fundamental resonant frequency of $f_o = 5.6$ GHz and fabricated on an RT/Duriod 6010.2 substrate with a thickness $h = 25$ mil and a relative dielectric constant $\varepsilon_r = 10.2$. The dimensions of the ring are $l_f = 5$ mm, $l_r = 20.34$ mm, and $w_1 = 0.6$ mm.

The equivalent ring circuit shown in Fig. 4 is divided by the input and output ports to form a shunt circuit denoted by the upper and lower parts, respectively. The equivalent circuits of the 45° mitered bend are represented by the inductor L and capacitor C[11] which are expressed by

$$C = 0.001h\left[(3.39\varepsilon_r + 0.62)\left(\frac{w_1}{h}\right)^2 + 7.6\varepsilon_r + 3.8\left(\frac{w_1}{h}\right)\right] \text{ pF} \quad (2a)$$

$$L = 0.22h\left\{1 - 1.35\exp\left[-0.18\left(\frac{w_1}{h}\right)^{1.39}\right]\right\} \text{ nH} \quad (2b)$$

where h and w_1 are in millimeters. The capacitance jB_T is the T-junction effect between the feed line and ring resonator

[1]*IE3D*, ver. 8.0, Zeland Software, Fremont, CA, 2001.

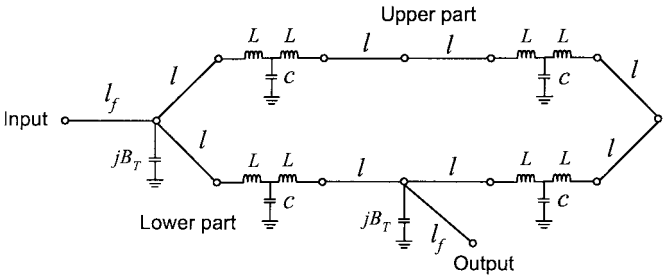

Fig. 4. Equivalent circuit of the ring using direct-connected orthogonal feed lines.

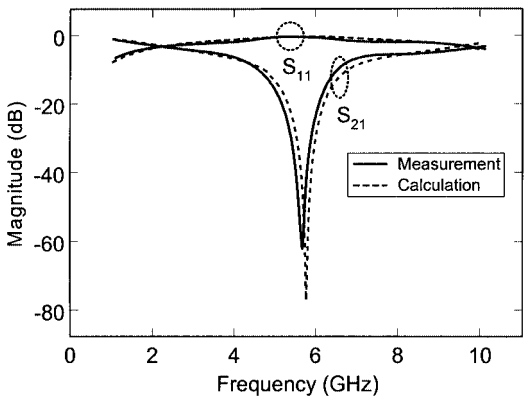

Fig. 5. Calculated and measured results of the ring using direct-connected orthogonal feed lines.

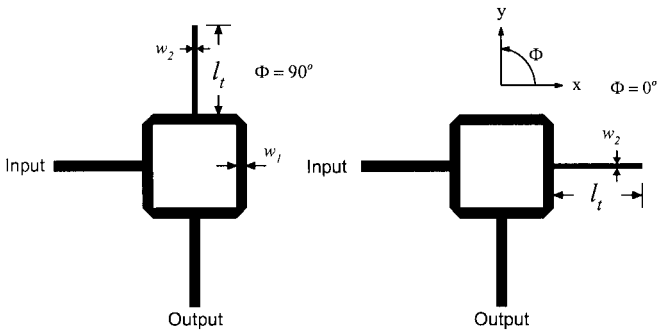

Fig. 6. Configuration of the ring with a tuning stub of $l_t = 5.03$ mm and $w_2 = 0.3$ mm at $\Phi = 90°$ or 0°.

[12]. The frequency response of the ring circuit can be calculated from the equivalent ring circuit using $ABCD$-, Y-, and S-parameters. Fig. 5 shows the calculated and measured results with good agreement.

B. One Tuning Stub

The effect of adding a tuning stub on the gap-coupled ring resonator has been discussed [1]. By changing the size or length of the tuning stub, the frequency response of the ring resonator is varied. Fig. 6 illustrates the orthogonal-feed ring resonator with a tuning stub of $l_t = \lambda_g/4$ designed at the center frequency and placed at the center of either side of the ring resonator. Furthermore, the ring resonator with one tuning stub forms an asymmetric configuration and will excite degenerate modes. The higher impedance of the tuning stub (w_2 for 50 Ω $< w_1$ for 64 Ω) is designed for a better return loss of the filter using two tuning stubs that will be shown in Section II-C.

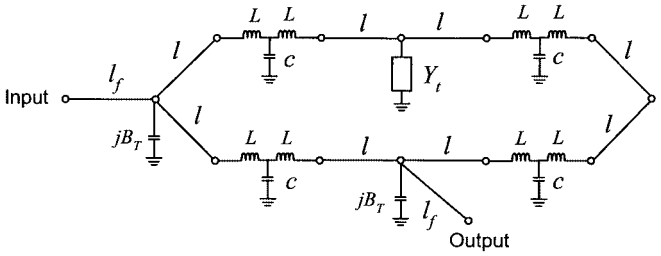

Fig. 7. Equivalent circuit of the ring using a tuning stub at $\Phi = 90°$.

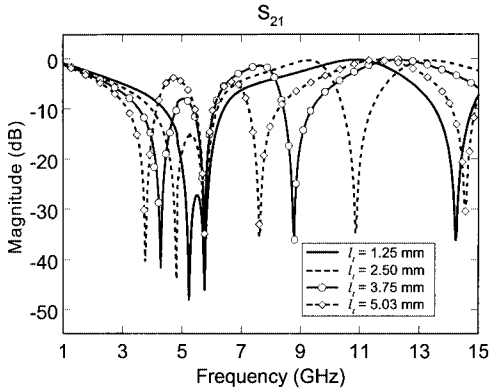

Fig. 8. Calculated results of the ring with various lengths of the tuning stub at $\Phi = 90°$.

Fig. 7 shows the equivalent circuit of the ring circuit with the tuning stub at $\Psi = 90°$. Y_t is the admittance looking into the tuning stub and can be expressed by

$$Y_t = y_0 \tanh(\gamma l_t + l_{\text{open}}) + jB_{T1} \tag{3}$$

where y_o is the characteristic admittance of the tuning stub, γ is the complex propagation constant, l_{open} is the equivalent open-effect length [13], and jB_{T1} is the capacitance of the T-junction between the ring and tuning stub l_t. The frequency response of the ring circuit can be obtained from the equivalent circuit by using $ABCD$-, Y-, and S-parameter calculations. Fig. 8 shows the calculated results for the different lengths of the tuning stub located at $\Phi = 90°$. Inspecting the results, when the length of the tuning stub increases, the degenerate modes of the ring at the fundamental and third modes are excited and moved to the lower frequencies. In addition, at the length of $l_t = \lambda_g/4 = 5.03$ mm, the ring circuit has three attenuation poles, as shown in Fig. 9. Comparing the frequency response to that of the ring circuit without the tuning stub in Fig. 5, the two additional degenerate modes are induced by the $\lambda_g/4$ tuning stub. The three attenuation poles are $f_1 = 3.81$ GHz with -39 dB rejection, $f_o = 5.77$ GHz GHz with -36 dB rejection, and $f_2 = 7.75$ GHz with -37 dB rejection. Furthermore, inspecting the ring resonators with the tuning stub at $\Phi = 90°$ or $\Phi = 0°$ in Fig. 6, S_{21} is the same for both cases due to the symmetry between these reciprocal networks.

C. Two Tuning Stubs

Fig. 10 shows the layout of the ring resonator with two tuning stubs of length $l_t = \lambda_g/4$ at $\Phi = 90°$ and $\Phi = 0°$. This symmetric ring circuit is divided by the tuning stubs and the input/output ports into four equal sections. The ring circuit can be treated as a combination of both perturbed ring circuits given in Fig. 6. By changing the lengths of two tuning stubs, the frequency response of the ring circuit will also be varied. Observing the calculated results in Fig. 11, two attenuation poles starting from the center frequencies of the fundamental and third modes move to the lower frequencies and form a wide passband. The measured and calculated results of the filter with the tuning stubs of length $\lambda_g/4$ are shown in Fig. 12. In addition, due to the symmetric structure, the ring circuit in Fig. 10 only excites a single mode.

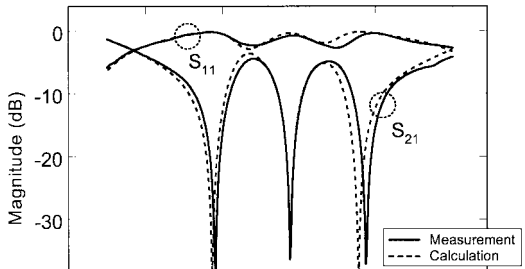

Fig. 9. Calculated and measured results of the ring using a tuning stub at $\Phi = 90°$.

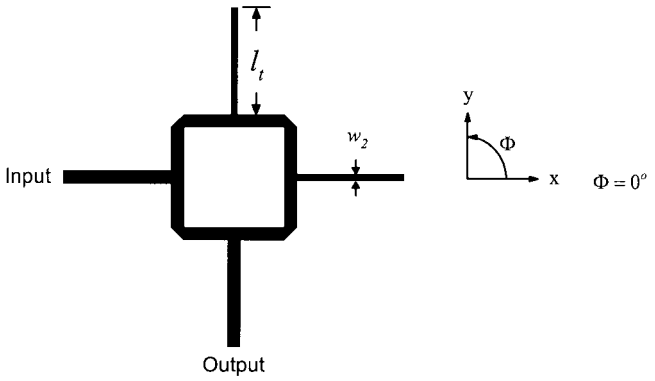

Fig. 10. Layout of the ring using two tuning stubs at $\Phi = 90°$ and $0°$.

Comparing the results in Fig. 12 with those in Fig. 9, the effects of adding two tuning stubs with a length of $l_t = \lambda_g/4$ at $\Phi = 90°$ and $\Phi = 0°$ provide a sharper cutoff frequency response, increase attenuations, and obtain a wide passband. Two attenuation poles are $f_1 = 3.81$ GHz with -46 dB rejection and $f_2 = 7.75$ GHz with -51 dB rejection. The differences between the measurement and calculation on f_1 and f_2 are due to fabrication tolerances that cause a slightly asymmetric layout and excite small degenerate modes.

The key point behind this new filter topology is that two tuning stubs loaded on the ring resonator at $\Phi = 90°$ and $\Phi = 0°$ are used to achieve a wide passband with a sharp cutoff characteristic. This approach can, in fact, be interpreted as using two stopbands induced by two tuning stubs in conjunction with the wide passband. In some cases, an undesired passband below the main passband may require a high passband section to be used in conjunction with this approach.

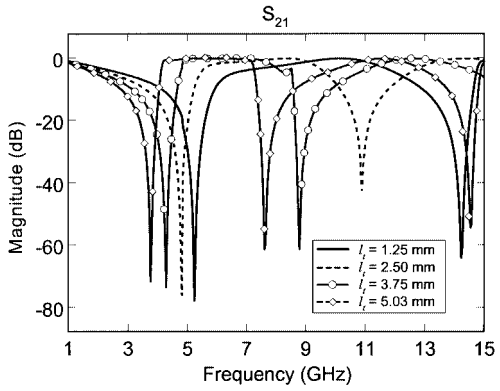

Fig. 11. Calculated results of the ring with various lengths of the tuning stub at $\Phi = 90°$ and $0°$.

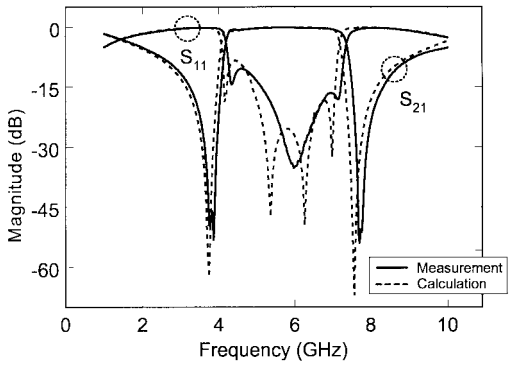

Fig. 12. Calculated and measured results of the ring with two tuning stubs of $l_t = \lambda_g/4 = 5.026$ mm at $\Phi = 90°$ and $0°$.

III. Wide-Band Microstrip Bandpass Filters With Dual-Mode Effects

Observing the frequency response in Fig. 12, the two stopbands of the filter show a narrow bandwidth. To increase the narrow stopbands, a dual-mode design can be used [1]. A square perturbation stub at $\Phi = 45°$ on the ring resonator is incorporated in Fig. 13(a). The square stub perturbs the fields of the ring resonator so that the resonator can excite a dual mode around the stopbands in order to improve the narrow stopbands. By increasing (decreasing) the size of the square stub, the distance (stopband bandwidth) between two modes is increased (decreased). The equivalent circuits of the square stub and the filter are displayed in Fig. 13(b) and (c), respectively. As seen in Fig. 13(b), the geometry at the corner of $\Phi = 45°$ is approximately equal to the square section of width $w_1 + w_p$, subtracting an isometric triangle of height w_1. The equivalent $L - C$ circuit of this approximation is also shown in Fig. 12(c), where $C_{\rm pf} = C_r - C$ and $L_p = LL_r/(L - L_r)$. The equivalent capacitance and inductance of the right-angle bend, C_r and L_r, are given by [11]

$$C_r = 0.001h\left[(10.35\varepsilon_r + 2.5)\left(\frac{w_1 + w_p}{h}\right)^2 + 2.6\varepsilon_r + 5.64\left(\frac{w_1 + w_p}{h}\right)\right] \text{ pF} \quad (4a)$$

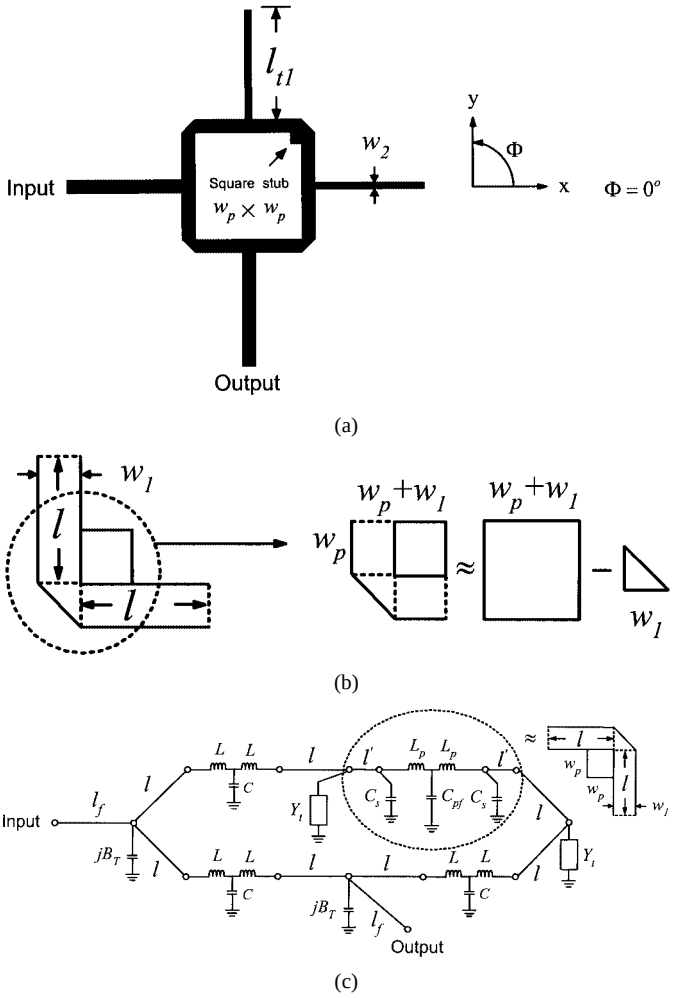

Fig. 13. Dual-mode filter. (a) Layout. (b) Equivalence of the perturbed stub. (c) Overall equivalent circuit.

$$L_r = 0.22h\left\{1 - 1.35\exp\left[-0.18\left(\frac{w_1 + w_p}{h}\right)^{1.39}\right]\right\} \text{ nH.} \quad (4b)$$

The asymmetric step capacitance C_s is [14]

$$C_s = w_p(0.012 + 0.0039\varepsilon_r) \text{ pF.} \quad (5)$$

In the above equations, all lengths are in millimeters. The length of the tuning stubs and size of the square stub are $l_{t1} = 4.83$ mm and $w_p \times w_p = 0.5 \times 0.5$ mm^2.

The calculated and measured results of the filter are shown in Fig. 14. As seen in Fig. 14, the square stub generates two transmission zeros (which are marked as $\times$ in Fig. 14) or dual modes located on either side of the passband at 3.66 and 7.62 and 7.62 and 8.07 GHz, respectively. Comparing S_{21} with that in Fig. 10, the dual-mode effects or transmission zeros increase the stopband bandwidth and also improve the return loss in the edges of the passband. The filter has 3-dB fractional bandwidth of 51.6%, an insertion loss of better than 0.7 dB, two rejections of greater than 18 dB within 3.43–4.3 GHz and 7.57–8.47 GHz, and an attenuation rate for the sharp cutoff frequency responses of 137.58 dB/GHz (calculated from 4.173 GHz with -36.9 dB to 4.42 GHz with -2.85 dB) and 131.8 dB/GHz (calculated

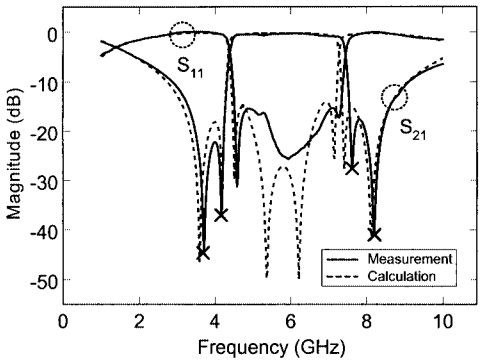

Fig. 14. Calculated and measured results of the dual-mode ring filter. The crosses (x) show the two transmission zero locations.

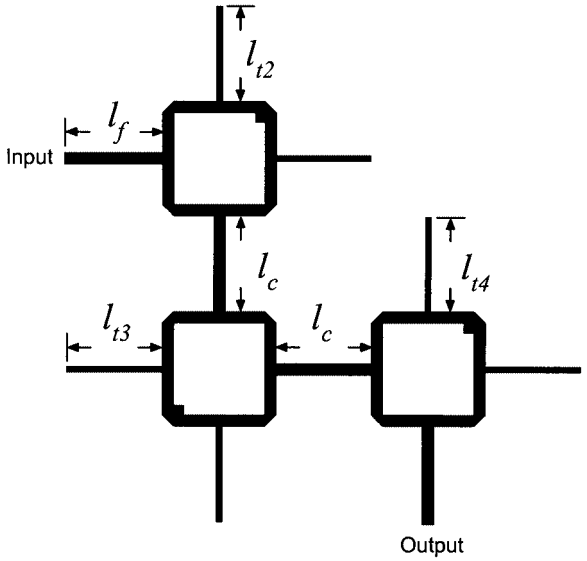

Fig. 15. Configuration of the cascaded dual-mode ring resonator.

from 7.44 GHz with 3.77 dB to 7.62 GHz with −27.5 dB). In addition, comparing the new filter with some compact and low insertion-loss filters [15], [16], those filters only show gradual rejections. To obtain a sharp cutoff frequency response, the filters need to increase numbers of resonators. However, increasing numbers of resonators increases the insertion loss and the size of the filter and also narrows the passband bandwidth [17], [18].

To obtain a higher rejection, a filter using three cascaded ring resonators is shown in Fig. 15. In this configuration, the three ring resonators are connected by a short transmission line of length $l_c = \lambda_g/4 = 4.89$ mm. The different length $l_{t2} = 4.85$ mm, $l_{t3} = 4.88$ mm, and $l_{t4} = 4.83$ mm for the tuning stubs are optimized for a good return loss.

Fig. 16 shows the calculated and measured results. The calculation also uses the transmission-line model with $ABCD$-, Y-, and S-parameter operations. The 3-dB fractional bandwidth of the filter is 49.3%. The filter has an insertion loss better than 1.6 dB and return loss greater than 13.3 dB in the passband from 4.58 to 7.3 GHz. Two stopbands are located at 2.75–4.02 and

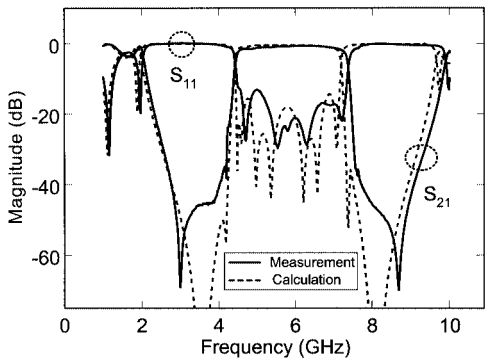

Fig. 16. Calculated and measured results of the cascaded dual-mode ring resonator filter.

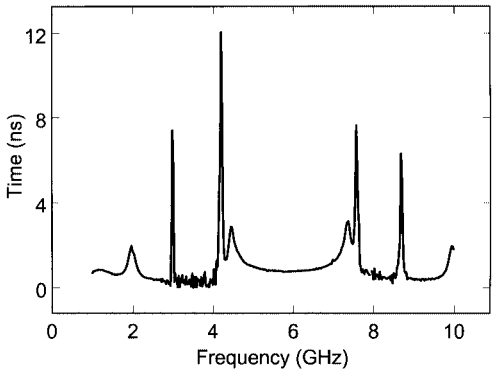

Fig. 17. Group delay of the cascaded dual-mode ring resonator filter.

7.73–9.08 GHz with rejection greater than 40 dB. The attenuation rate of the filter for the sharp cutoff frequency responses is 99.75 dB/GHz (calculated from 4.17 GHz with −34.9 dB to 4.49 GHz with −2.98 dB) and 101.56 dB/GHz (calculated from 7.32 GHz with −3.4 dB to 7.64 GHz with −35.9 dB). The group delay of this wide-band bandpass filter can be calculated by

$$\tau = -\frac{\partial \angle S_{21}}{\partial \omega} \tag{6}$$

where $\angle S_{21}$ is the insertion-loss phase and ω is the frequency in radians per second. Fig. 17 shows the group delay of the filter. Within the passband, the group delay is below 2 ns.

IV. Conclusions

A new compact, low insertion-loss, sharp-rejection, and wide-band microstrip bandpass filter has been developed. A bandstop filter using a ring resonator with direct-connected orthogonal feeders is introduced. Next, new filters are developed from the bandstop filter to achieve a wide-band passband and two sharp stopbands. A dual-mode design was also used to increase the widths of rejection bands. Without any coupling gaps between feed lines and rings, there are no mismatch and radiation losses between them. Therefore, the new filters show low insertion loss. Simple transmission-line models are used to calculate the frequency responses of the new filters. The measurements agree well with the calculations. The new filters were designed for mitigating the interference in full duplex systems in satellite communications.

ACKNOWLEDGMENT

The authors would like to thank C. Wang, Texas A&M University, College Station, for his technical assistance and C. Rodenbeck, Texas A&M University, for his helpful discussions.

REFERENCES

[1] K. Chang, *Microwave Ring Circuits and Antennas*. New York: Wiley, 1996.

[2] G. K. Gopalakrishnan and K. Chang, "Novel excitation schemes for the microstrip ring resonator with lower insertion loss," *Electron. Lett.*, vol. 30, no. 2, pp. 148–149, Jan. 1994.

[3] L.-H. Hsieh and K. Chang, "Compact dual-mode elliptic-function bandpass filter using a single ring resonator with one coupling gap," *Electron. Lett.*, vol. 36, no. 19, pp. 1626–1627, Sept. 2000.

[4] W. C. Jung, H. J. Park, and J. C. Lee, "Microstrip ring bandpass filters with new interdigital side-coupling structure," in *Asia–Pacific Microwave Conf.*, vol. 3, 1999, pp. 678–681.

[5] L. Zhu and K. Wu, "A joint field/circuit model of line-to-ring coupling structures and its application to the design of microstrip dual-mode filters and ring resonator circuits," *IEEE Trans. Microwave Theory Tech*, vol. 47, pp. 1938–1948, Oct. 1999.

[6] M. Matsuo, H. Yabuki, and M. Makimoto, "Dual-mode stepped-impedance ring resonator for bandpass filter applications," *IEEE Trans. Microwave Theory Tech.*, vol. 49, pp. 1235–1240, July 2001.

[7] L.-H. Hsieh and K. Chang, "Dual-mode quasi-elliptic-function bandpass filters using ring resonators with enhanced-coupling tuning stubs," *IEEE Trans. Microwave Theory Tech.*, vol. 50, pp. 1340–1345, May 2002.

[8] J. S. Hong, M. Lancaster, D. Jedamzik, and R. B. Greed, "On the development of superconducting microstrip filters for mobile communications applications," *IEEE Trans. Microwave Theory Tech.*, vol. 47, pp. 1656–1663, Sept. 1999.

[9] L.-H. Hsieh and K. Chang, "Slow-wave bandpass filters using ring or stepped-impedance hairpin resonators," *IEEE Trans. Microwave Theory Tech.*, vol. 50, pp. 1795–1800, July 2002.

[10] D. K. Paul, P. Gardner, and K. P. Tan, "Suppression of even modes in microstrip ring resonators," *Electron. Lett.*, vol. 30, no. 30, pp. 1772–1774, Oct. 1994.

[11] M. Kirschning, R. H. Jansen, and N. H. L. Koster, "Measurement and computer-aided modeling of microstrip discontinuities by an improved resonator method," in *IEEE MTT-S Int. Microwave Symp. Dig.*, 1983, pp. 495–497.

[12] E. Hammerstad, "Computer-aided design for microstrip couplers with accurate discontinuity models," in *IEEE MTT-S Int. Microwave Symp. Dig.*, 1981, pp. 54–56.

[13] K. C. Gupta, R. Garg, I. Bahl, and P. Bhartia, *Microstrip Lines and Slotlines*, 2nd ed. Norwood, MA, 1996, p. 181.

[14] B. C. Wadell, *Transmission Line Design Handbook* Norwood, MA, 1991, p. 321.

[15] L. Zhu, H. Bu, and K. Wu, "Broadband and compact multi-pole microstrip bandpass filters using ground plane aperture technique," *Proc. Inst. Elect. Eng.*, pt. H, vol. 149, no. 1, pp. 71–77, Feb. 2002.

[16] J. -S. Park, J.-S. Yun, and D. Ahn, "A design of the novel coupled-line bandpass filter using defected ground structure with wide stopband performance," *IEEE Trans. Microwave Theory Tech.*, vol. 50, pp. 2037–2043, Sept. 2002.

[17] J. J. Yu, S. T. Chew, M. S. Leong, and B. L. Ooi, "New class of microstrip miniaturized filter using triangular stub," *Electron. Lett.*, vol. 37, no. 37, pp. 1169–1170, Sept. 2001.

[18] J.-R. Lee, J.-H. Cho, and S.-W. Yun, "New compact bandpass filter using microstrip 1/4 resonators with open stub inverter," *IEEE Wireless Comp. Lett.*, vol. 10, pp. 526–527, Dec. 2000.

Lung-Hwa Hsieh (S'01) was born in Panchiao, Taiwan, R.O.C., in 1969. He received the B.S. degree in electrical engineering from Chung Yuan Christian University, Chungli, Taiwan, R.O.C., in 1991, the M.S. degree in electrical engineering from the National Taiwan University of Science and Technology, Taipei, Taiwan, R.O.C., in 1993, and is currently working toward the Ph.D. degree in electrical engineering at Texas A&M University, College Station.

From 1995 to 1998, he was a Senior Design Engineer with General Instrument, Taipei, Taiwan, R.O.C., where he was involved in RF video and audio circuit design. Since 2000, he has been a Research Assistant with the Department of Electrical Engineering, Texas A&M University. His research interests include microwave integrated circuits and devices.

Kai Chang (S'75–M'76–SM'85–F'91) received the B.S.E.E. degree from the National Taiwan University, Taipei, Taiwan, R.O.C., in 1970, the M.S. degree from the State University of New York at Stony Brook, in 1972, and the Ph.D. degree from The University of Michigan at Ann Arbor, in 1976.

From 1972 to 1976, he was with the Microwave Solid-State Circuits Group, Cooley Electronics Laboratory, The University of Michigan at Ann Arbor, where he was a Research Assistant. From 1976 to 1978, he was with Shared Applications Inc., Ann Arbor, MI, where he was involved with computer simulation of microwave circuits and microwave tubes. From 1978 to 1981, he was with the Electron Dynamics Division, Hughes Aircraft Company, Torrance, CA, where he was involved in the research and development of millimeter-wave solid-state devices and circuits, power combiners, oscillators, and transmitters. From 1981 to 1985, he was with TRW Electronics and Defense, Redondo Beach, CA, where he was a Section Head involved with the development of state-of-the-art millimeter-wave integrated circuits and subsystems, including mixers, voltage-controlled oscillators (VCOs), transmitters, amplifiers, modulators, upconverters, switches, multipliers, receivers, and transceivers. In August 1985, he joined the Electrical Engineering Department, Texas A&M University, College Station, as an Associate Professor, and became a Professor in 1988. In January 1990, he became an E-Systems Endowed Professor of Electrical Engineering. He has authored and coauthored several books, including *Microwave Solid-State Circuits and Applications* (New York: Wiley, 1994), *Microwave Ring Circuits and Antennas* (New York: Wiley, 1996), *Integrated Active Antennas and Spatial Power Combining* (New York: Wiley, 1996), and *RF and Microwave Wireless Systems* (New York: Wiley, 2000). He has served as the Editor of the four-volume *Handbook of Microwave and Optical Components* (New York: Wiley, 1989 and 1990). He is the Editor of *Microwave and Optical Technology Letters* and the Wiley Book Series on "Microwave and Optical Engineering." He has also authored or coauthored over 350 technical papers and several book chapters in the areas of microwave and millimeter-wave devices, circuits, and antennas. His current interests are microwave and millimeter-wave devices and circuits, microwave integrated circuits, integrated antennas, wide-band and active antennas, phased arrays, microwave power transmission, and microwave optical interactions.

Dr. Chang was the recipient of the 1984 Special Achievement Award presented by TRW, the 1988 Halliburton Professor Award, the 1989 Distinguished Teaching Award, the 1992 Distinguished Research Award, and the 1996 Texas Engineering Experiment Station (TEES) Fellow Award presented by Texas A&M University.